

DOI: 10.19663/j.issn2095-9869.20220507001

http://www.yykxjz.cn/

周启苓, 王刘永, 杨云生, 马骞, 吴雨薇, 陈刚. 不同发育期虹鳟脊椎骨的显微结构及钙、磷元素含量分析. 渔业科学进展, 2023, 44(5): 115–124

ZHOU Q L, WANG L Y, YANG Y S, MA Q, WU Y W, CHEN G. Calcium and phosphorus contents, and microstructure of vertebrae in rainbow trout (*Oncorhynchus mykiss*) at different developmental stages. Progress in Fishery Sciences, 2023, 44(5): 115–124

## 不同发育期虹鳟脊椎骨的显微结构 及钙、磷元素含量分析\*

周启苓<sup>1</sup> 王刘永<sup>1</sup> 杨云生<sup>1</sup> 马骞<sup>1,2①</sup> 吴雨薇<sup>1</sup> 陈刚<sup>1,2</sup>

(1. 广东海洋大学水产学院 广东 湛江 524088;

2. 南方海洋科学与工程广东省实验室(湛江) 广东 湛江 524025)

**摘要** 为揭示虹鳟(*Oncorhynchus mykiss*)脊椎骨的形态结构、元素组成等特征在生长发育过程中的变化情况,本研究分别采集4个发育期(分别为幼鱼I期、幼鱼II期、成鱼I期和成鱼II期,平均体质量分别为4、35、644和2 129 g)的虹鳟脊椎骨样品,利用电感耦合等离子体质谱(ICP-MS)检测其第1~6节脊椎骨中钙、磷元素含量,并运用显微CT(Micro-CT)技术对其第4~6节脊椎骨进行扫描与三维重建。结果显示,虹鳟第1~6节脊椎骨的钙、磷元素含量在不同发育期均呈先升高后降低的趋势,脊椎骨中钙、磷元素含量在幼鱼II期最高;脊椎骨钙/磷摩尔质量比在生长发育过程中显著增加。第4~6节脊椎骨的显微结构扫描结果显示,脊椎骨的骨小梁数量(trabecular number, Tb.N)随虹鳟的生长呈显著降低趋势;骨小梁厚度(trabecular thickness, Tb.Th)和骨小梁分离度(trabecular separation/spacing, Tb.Sp)在生长发育过程中显著增加;脊椎骨的骨体积分数(bone volume fraction, BV/TV)、组织矿物质密度(tissue mineral density, TMD)和骨矿物质密度(bone mineral density, BMD)等指标均在成鱼I期中最低,其次为幼鱼II期;脊椎骨中BV/TV及TMD在成鱼II期中最高,而BMD在幼鱼I期中最大。上述结果不仅为虹鳟发育生物学研究提供了基础数据,还可为鱼类年龄鉴定和分类鉴定等研究提供理论依据。

**关键词** 虹鳟; 脊椎骨; 生长发育; 显微结构; 元素含量

**中图分类号** S917.4 **文献标识码** A **文章编号** 2095-9869(2023)05-0115-10

虹鳟(*Oncorhynchus mykiss*)是联合国粮农组织(FAO)在世界范围内推广的优质淡水养殖品种之一(曹祥栋, 2017);同时是我国养殖产量最高的鲑鳟鱼类,在我国青海、甘肃、辽宁和山东等地均有大规模的养殖。近年来,国内外学者对虹鳟开展了大量研究,旨在筛选虹鳟适宜的养殖条件(Akhan *et al*, 2010)、明

确其合理的营养需求(Bordignon *et al*, 2022),并针对病害进行精准诊断及治疗(Sönmez *et al*, 2021)。然而,针对虹鳟骨骼相关的基础研究较少,主要是关于人工养殖虹鳟骨骼畸形类型的研究(Deschamps *et al*, 2008; Jagiełło *et al*, 2021),未发现与其骨骼结构方面相关的研究。

\* 国家自然科学基金项目(31772828)和广东海洋大学科研启动经费资助项目(R19022)共同资助。周启苓, E-mail: 18738627206@163.com

① 通信作者: 马骞, 副教授, E-mail: maq@gdou.edu.cn

收稿日期: 2022-05-07, 收修改稿日期: 2022-05-23

鱼类骨骼系统由主轴骨骼(头骨、脊柱、肋骨和肌间骨)和附肢骨骼组成,对运动、摄食、躲避敌害、发育和承重等行为及生理功能至关重要(孟庆闻等, 1987; Hu *et al.*, 2019)。硬骨鱼类的脊柱由许多脊椎骨自头后到尾基相互连接而成,其中最主要的矿物元素为钙和磷。已有研究表明,鱼类脊椎骨的形态结构及钙、磷等元素含量在不同鱼类中存在一定的差异,在自仔稚鱼到成鱼的不同发育时期也有明显变化,因此,可依据上述信息进行年龄鉴定、分类鉴定甚至鱼类的生活史鉴定等工作(陈咏霞等, 2014; 谢玺等, 2021)。然而,目前尚未见对不同发育时期硬骨鱼类脊柱形态结构及元素含量的相关研究。

脊椎动物骨骼结构研究中较为常见的方法有双能 X 线吸收测定法(DXA)、定量 CT 测量法(QCT)、定量超声技术(QUS)和显微 CT 技术(Micro-CT)等, Micro-CT 是其中最高级的应用分析技术。Micro-CT 扫描技术的原理是利用 X 射线在不同物质中穿透能力不同的特质,通过计算从不同方向发射到物体上的 X 射线衰减程度,对个体进行扫描、三维重建及显微结构指标分析(刘广鹏, 2006; 张扬等, 2005)。Micro-CT 扫描技术具有空间分辨率高、成本低廉、使用方便等优点,自 Feldkamp 等(1989)将其首次应用于骨骼结构研究后,因其能准确测量不同骨组织的骨矿物质密度(bone mineral density, BMD)等指标(魏占英等, 2018; Bouxsein *et al.*, 2010),在骨形态和骨微结构等研究领域获得广泛应用。近年来,国内外学者应用该技术对鱼类骨骼结构开展了少量研究工作。例如,张宁等(2012)利用 Micro-CT 对鲤(*Cyprinus carpio*)分析发现,不同部位骨骼的显微结构指标具有显著差异,推测可能与其运动和骨骼的复杂程度有关;王映等(2016)利用 Micro-CT 对大黄鱼(*Larimichthys crocea*)养殖群体和野生群体的脊椎骨显微结构进行了比较分析;李晓慧等(2020)利用 Micro-CT 扫描分析发现,两水系的花斑裸鲤(*Gymnocypris eckloni Herzenstein*)在背鳍支鳍骨插入椎骨间的相对位置上存在极显著差异( $P < 0.01$ ),或许可作为对其进行分类鉴定的依据。

电感耦合等离子体质谱(ICP-MS)是一种高精度、高灵敏度、准确高效的元素定量分析技术,在生物、医学、食品、环境等领域具有广泛应用(黄丹宇等, 2021; 曾涛等, 2018)。近年来,该技术也被应用于鱼类骨骼、肌肉等组织中微量元素的检测。例如,梁键钧(2012)利用该技术对草鱼(*Ctenopharyngodon idella*)幼鱼全鱼、脊椎骨和鳞片中的钙、磷元素含量进行了检测,以分析其对饲料中各矿物质水平的需

求;王硕等(2010)利用 ICP-MS 对多种海产品中的不同金属元素含量进行了检测;郑红艳等(2017)利用该技术测定了草鱼、乌鳢(*Channa argus*)等十几种水生动物体内的铜、镉等重金属元素的含量。

目前,关于虹鳟骨骼系统的研究多集中在人工养殖环境下的骨骼畸形类型(Camp, 2021; Deschamps *et al.*, 2008、2009)及盐度驯化对骨代谢的影响等方面(Zhou *et al.*, 2022)。为揭示虹鳟脊椎骨在生长发育过程中的形态结构等特征,本研究分别利用 Micro-CT 及 ICP-MS 技术对其不同发育期脊椎骨进行三维结构扫描重建、显微结构指标分析及钙、磷元素含量检测,通过比较其形态结构及元素含量的差异,探讨骨骼形态在发育过程中的变化情况,相关结果既可丰富虹鳟骨骼结构的基础数据,还可为鱼类分类鉴定和年龄鉴定等研究提供理论依据。

## 1 材料与方法

### 1.1 实验材料

实验鱼于 2021 年 6 月采集自甘肃省临夏市九眼泉虹鳟鱼场。养殖水温( $11 \pm 1$ ) °C、水深 1 m、溶解氧 4.7~8.8 mg/L、养殖密度 25 kg/m<sup>3</sup>。养殖期间,采用人工投饵的方式投喂天邦鲑鳟鱼饲料,幼鱼 I 期每日投饵 4~5 次,幼鱼 II 期每日投饵 3~4 次,成鱼 I 期和成鱼 II 期每日投饵 1~2 次。水温低于 22 °C 时,按照体重百分比投饵;水温高于 22 °C 时,采用饱食投饵。选取健康有活力、体型均匀的不同发育期虹鳟,稚鱼期的体质量为( $1.27 \pm 0.21$ ) g,体长为( $3.05 \pm 0.35$ ) cm;幼鱼 I 期的体质量为( $4.57 \pm 0.96$ ) g,体长为( $8.45 \pm 1.40$ ) cm;幼鱼 II 期的体质量为( $35.79 \pm 4.35$ ) g,体长为( $25.65 \pm 1.70$ ) cm;成鱼 I 期的体质量为( $644.37 \pm 109.76$ ) g,体长为( $32.50 \pm 2.20$ ) cm;成鱼 II 期的体质量为( $2\ 129.25 \pm 412.75$ ) g,体长为( $48.75 \pm 6.25$ ) cm,各 6 尾。

### 1.2 虹鳟脊椎骨形态特征分析

取 6 尾稚鱼期虹鳟进行麻醉后,采用软骨-硬骨双染色法(Dingerkus *et al.*, 1977)对其进行全鱼骨骼染色,利用 Leica M205 FCA 体视显微镜对透明标本进行观察并拍照(鱼体左侧俯拍)。

取 3 尾成鱼 I 期虹鳟进行麻醉后,利用宠物 X 射线扫描(X-ray Scanner)技术对全鱼骨骼进行扫描拍摄(鱼体左侧俯拍),仪器参数设定:电压 54 kV,电流 100 mA,曝光时间 63 ms。

### 1.3 虹鳟脊椎骨的 Micro-CT 扫描分析

对不同发育期的虹鳟个体及其脊椎骨进行编号, 利用 Micro-CT ( $\mu$ CT100, Scanco Medical AG, 瑞士) 分别对不同个体的第 4~6 节脊椎骨进行逐节扫描。每个脊椎骨样品置入标本管后, 使用医用纱布填充样品周围间隙, 并在标本管中加入 70%乙醇作为扫描介质。

扫描条件: 电压 70 kV、电流 200  $\mu$ A, 360°旋转扫描、旋转角增量 0.4°。对于不同发育期虹鳟的脊椎骨样品, 依据样品大小选取能达到最高扫描分辨率的扫描参数(表 1)。最后, 利用  $\mu$ CT Ray V4.2 图像处理软件分别对不同个体的第 4~6 节脊椎骨进行三维重建。

表 1 4 个不同发育期虹鳟脊椎骨的 Micro-CT 扫描参数

Tab.1 Micro-CT scanning parameters of *O. mykiss* vertebrae at four different developmental stages

样品 Sample	分辨率 Resolution ratio/ $\mu$ m	图片像素 Image pixel	扫描时间 Scanning time/min	截面数量 Section number
幼鱼 I 期 Young stage I	6.6	3 072×3 072	30	431
幼鱼 II 期 Young stage II	7.4	2 048×2 048	36	601
成鱼 I 期 Adult stage I	14.0	2 510×2 510	57	881
成鱼 II 期 Adult stage II	14.0	2 510×2 510	60	1 657

采用  $\mu$ CT Evaluation Program V6.6 软件分别对不同个体的第 4~6 节脊椎骨样品的扫描结果进行检测分析, 检测指标: 组织体积(tissue volume, TV)、骨体积(bone volume, BV)、骨小梁厚度(trabecular thickness, Tb.Th)、骨小梁数量(trabecular number, Tb.N)、骨小梁分离度(trabecular separation/spacing, Tb.Sp)、BMD 和组织矿物质密度(tissue mineral density, TMD)等(安晓等, 2018; 魏占英等, 2018; Pinto *et al.*, 2010)。其中, Tb.Th、Tb.N、Tb.Sp 和 SMI 为骨小梁空间形态结构的评价指标, BMD 为骨骼强度评价指标。

### 1.4 虹鳟脊椎骨中钙、磷元素含量检测

选取用于 Micro-CT 扫描分析的相同虹鳟个体, 将其第 1~6 节脊椎骨取出并清理表面肌肉, 进行初步破碎后置于 V (氯仿): V (甲醇)=1:1 溶液中完全浸没 24 h, 再经超纯水反复浸泡、清洗, 在烘箱中(105  $^{\circ}$ C)烘干 12 h 后, 研磨成粉待用(梁键钧, 2012; Markvart *et al.*, 2012)。取每个样品的脊椎骨粉末约 0.1 g, 置于加有 6 mL HCl-HNO<sub>3</sub>-HF-H<sub>2</sub>O<sub>2</sub> (3:1:1:1)溶液的聚四氟乙烯容器中, 并在微波炉中消解(Zhou *et al.*, 2022)。随后, 将聚四氟乙烯容器在加热块(180  $^{\circ}$ C)上去除余酸(Wang *et al.*, 2017)。将消解液转移至离心管中, 用超纯水至少冲洗容器壁 3 次, 容器中残留的消解液一并转移, 最后用超纯水定容至 50 mL。将定容后的消解液用超纯水稀释后上机测定, 通过空白酸校正系统误差。利用 ICP-MS(Agilent 7500 Cx, 美国)测定各样品消解液中钙、磷含量, 并计算钙/磷质量比和钙/磷(摩尔质量比值)(表示磷酸钙的结晶相, 例如, 纯羟基磷灰石钙中的理论钙/磷(摩尔质量比值)为 1.67。

所有样品均设置 3 个重复, 消解并使用标准物质

GBW10024(扇贝生物成分分析标准物质, GSB-15)进行校准。为了避免潜在的污染, 使用不锈钢工具处理脊椎骨样品, 并及时使用超纯水清洗。本研究使用的所有化学品均为特级试剂(GR)(上海安谱实验科技股份有限公司)。使用前, 所有玻璃器皿均在 20%硝酸中浸泡至少 24 h, 并使用超纯水冲洗至少 3 次。同时进行空白和对照标准实验, 对实验结果进行校正。上述钙、磷元素含量检测由广东海洋大学分析测试中心完成。

### 1.5 统计分析

数据经 Excel 2019 软件初步整理后, 使用 SPSS 19.0 软件进行独立样本 *t* 检验分析。所有值均使用平均值 $\pm$ 标准误(Mean $\pm$ SE)表示,  $P < 0.05$  具有显著性差异。

## 2 结果与分析

### 2.1 虹鳟稚鱼与成鱼全鱼骨骼结构

虹鳟稚鱼全骨骼染色结果见图 1A。可以看出, 脊椎骨在该发育期已骨化完全。结合成鱼全鱼 X 射线扫描结果可知(图 1B), 虹鳟脊椎骨共计 63 节, 两端分别与头、尾相连; 肋骨附着在躯椎骨上, 自 1~33 躯椎骨的腹侧向下成弧形分开排列, 无肌间刺; 在脊椎骨背侧, 神经弓围绕神经管并与神经棘融合; 与肋骨不同, 尾椎骨有血管拱, 形成血管和神经的通道, 并在腹侧与血管棘融合。

### 2.2 不同发育期虹鳟脊椎骨显微结构

4 个不同发育期虹鳟第 4~6 节脊椎骨侧面观及第 4 节脊椎骨横截面图像如图 2A~H 所示。在同一发育

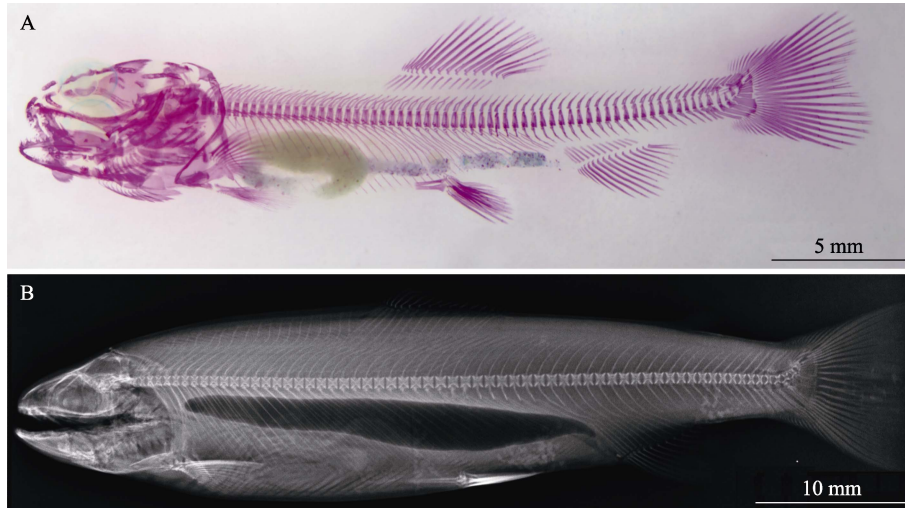


图1 虹鳟稚鱼及成鱼的全骨骼结构

Fig.1 Whole-body bone structure of juvenile and adult *O. mykiss*

A: 稚鱼期虹鳟全鱼骨骼; B: 成鱼 I 期虹鳟全鱼骨骼

A: Skeleton structure of juvenile *O. mykiss*; B: Skeleton structure of adult stage I *O. mykiss*

期,第4~6节脊椎骨在形态结构方面未见显著差异;第5节脊椎骨的三维扫描和重建结果(图3A~D)在不同发育期也较为相似。然而,脊椎骨的体积与面积均随虹鳟的生长显著增加,脊椎骨之间的分节更加明显,脊椎骨的结构更加充实完整。由不同发育期虹鳟脊椎骨显微结构指标的检测结果显示(表2),Tb.N随虹鳟的生长呈显著降低趋势( $P<0.05$ ),在幼鱼I期,每毫米脊椎骨中Tb.N最高,为 $(19.915\pm 0.758)$  ind./mm;在成鱼II期最低,为 $(1.960\pm 0.043)$  ind./mm。Tb.Th和Tb.Sp均随虹鳟的生长呈显著增加趋势( $P<0.05$ ),幼鱼I期虹鳟脊椎骨的Tb.Th和Tb.Sp最低,分别为 $(0.060\pm 0.001)$  mm和 $(0.068\pm 0.004)$  mm,成鱼II期脊椎骨Tb.Th和Tb.Sp最高,分别为 $(0.718\pm 0.026)$  mm和 $(0.402\pm 0.029)$  mm。BV/TV、TMD和BMD随虹鳟的生长呈先降低后升高的趋势,在成鱼I期脊椎骨中最低,分别为 $(62.620\pm 13.223)\%$ 、 $(460.300\pm 102.825)$  mg/mL和 $(678.052\pm 4.417)$  mg/mL;其次为幼鱼II期的虹鳟脊椎骨;在成鱼II期的虹鳟脊椎骨中BV/TV和TMD最高,分别为 $(86.473\pm 1.029)\%$ 和 $(654.797\pm 7.031)$  mg/mL;BMD在幼鱼I期脊椎骨中最大,为 $(820.527\pm 5.003)$  mg/mL。

### 2.3 不同发育期虹鳟脊椎骨中钙、磷元素含量

4个不同发育期虹鳟第1~6节脊椎骨钙、磷元素含量、钙/磷质量比及钙/磷(摩尔质量比值)见表3。脊椎骨中钙、磷含量在生长发育过程中呈先升高后降低的趋势,其中,幼鱼II期的虹鳟脊椎骨中钙、磷元素含量最高,分别为 $(4\ 711.121\pm 567.948)$ 和 $(3\ 649.488\pm$

$446.961)$   $\mu\text{mol/g}$ 。此外,脊椎骨中的钙/磷质量比和钙/磷(摩尔质量比值)均随虹鳟的生长呈显著升高趋势( $P<0.05$ )。

### 3 讨论

不同鱼类的脊椎骨数量和形态特征各异,上述差异可作为鱼类物种鉴定的重要依据之一。本研究中,虹鳟脊椎骨数目共计63节,其中,躯椎骨33节、尾椎骨30节;大西洋鲑(*Salmo salar*)(Fjellidal et al, 2012)脊椎骨数目通常为57~60节(30节躯椎骨,27~30节尾椎骨)。可见尽管上述2个鱼种同属鲑科(Salmonidae),但脊椎骨类型及其数目差异显著,可据此进行物种鉴别。对于脊椎骨数量较为相近的同属鱼类,则需通过骨骼形态特征进行进一步区分,例如,Huber等(2011)发现,可通过测量脊椎骨的长度、高度和长度/高度等参数对同属于太平洋鲑属(*Oncorhynchus*)的大鳞大麻哈鱼(*Oncorhynchus tshawytscha*)和克拉克大麻哈鱼(*O. clarkii*)进行区分;然而,上述参数在同属的其他鱼种间会存在测量数据重叠,难以对同属的所有鱼种进行有效鉴别。近年来,随着Micro-CT扫描技术在骨骼显微结构分析中的广泛应用,利用脊椎骨的三维结构作为鱼类分类鉴定的依据已有相关报道。Sakashita等(2019)利用Micro-CT扫描技术比较分析了32种硬骨鱼类(分属于10目)的同一节脊椎骨的三维结构,结果表明,第1个有脉棘融合的脊椎骨上的片状骨小梁和内部空腔结构在不同鱼类中存在显著差异,由此推测,这些结构特征可应用于鱼类的分类鉴定。

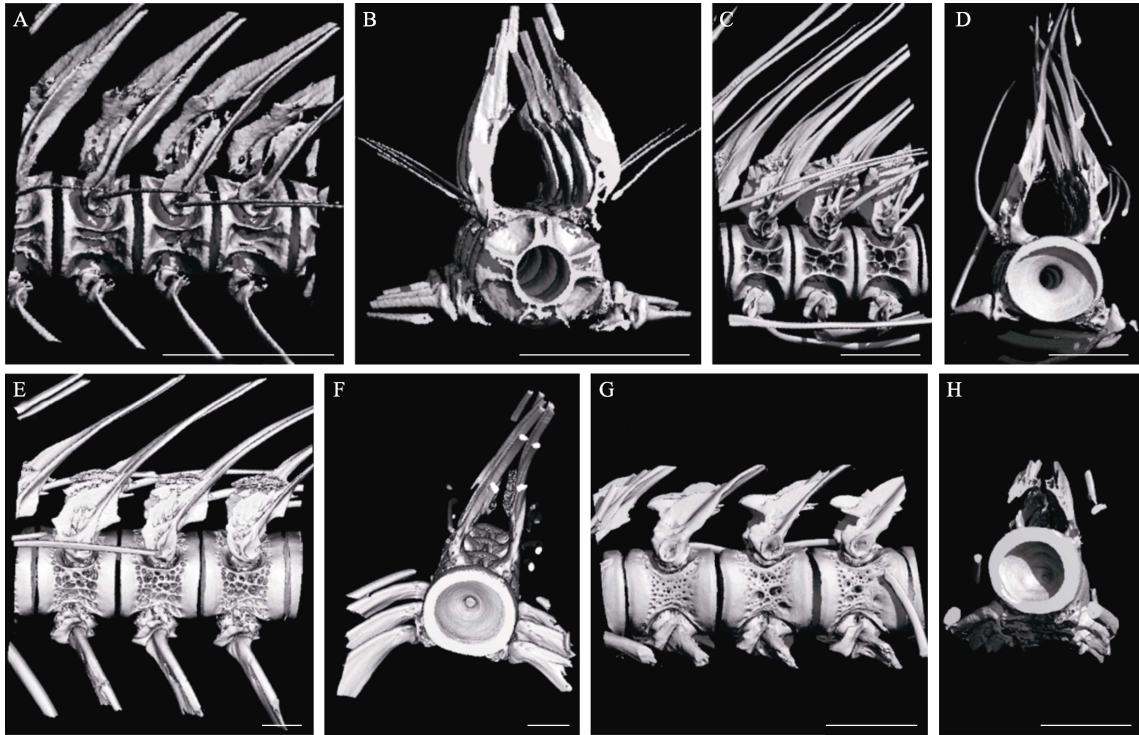


图 2 4 个不同发育期虹鳉第 4~6 节脊椎骨的三维扫描

Fig.2 Three-dimensional scanning of the 4~6th vertebrae in *O. mykiss* at four different developmental stages

A: 幼鱼 I 期脊椎骨侧面; B: 幼鱼 I 期第 4 节脊椎骨横截面; C: 幼鱼 II 期脊椎骨侧面; D: 幼鱼 II 期第 4 节脊椎骨横截面; E: 成鱼 I 期脊椎骨侧面; F: 成鱼 I 期第 4 节脊椎骨横截面; G: 成鱼 II 期脊椎骨侧面; H: 成鱼 II 期第 4 节脊椎骨横截面。比例尺是右下角的白色线条, A~F 的比例尺为 1.0 mm, G 和 H 的比例尺为 5.0 mm。

A: Lateral view of vertebrae collected at young stage I; B: Cross section view of the 4th vertebra collected at young stage I; C: Lateral view of vertebrae collected at young stage II; D: Cross section view of the 4th vertebra collected at young stage II; E: Lateral view of vertebrae collected at adult stage I; F: Cross section view of the 4th vertebra collected at adult stage I; G: Lateral view of vertebrae collected at adult stage II; H: Cross section view of the 4th vertebra collected at adult stage II. Scale bar was the white line in the lower right corner, A~F scale bar=1.0 mm, G and H scale bar=5.0 mm.

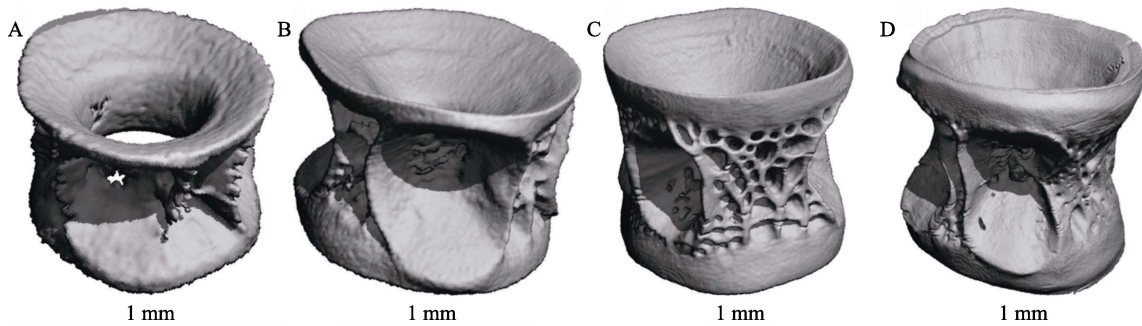


图 3 4 个不同发育期虹鳉第 5 节脊椎骨的三维重建

Fig.3 Three-dimensional reconstruction of the 5th vertebra in *O. mykiss* at four different developmental stages

A: 幼鱼 I 期脊椎骨; B: 幼鱼 II 期脊椎骨; C: 成鱼 I 期脊椎骨; D: 成鱼 II 期脊椎骨。

A: Vertebra of *O. mykiss* at young stage I; B: Vertebra of *O. mykiss* at young stage II; C: Vertebra of *O. mykiss* at adult stage I; D: Vertebra of *O. mykiss* at adult stage II.

鱼类骨骼矿化程度主要由其中钙、磷元素的含量表征, 其在不同鱼类中也具有一定的差异。据报道, 在 2~3 kg 规格的四大家鱼的脊椎骨中, 青鱼

(*Mylopharyngodon piceus*)钙/磷(摩尔质量比值)为 1.40, 草鱼脊椎骨钙/磷(摩尔质量比值)为 1.38, 鳊鱼(*Aristichthys nobilis*)为 1.27, 鲢鱼(*Hypophthalmichthys*

表2 4个不同发育期虹鳟脊椎骨显微结构检测指标

Tab.2 Comparison of micro structural vertebrae index of *O. mykiss* at four different developmental stages

指标 Index	幼鱼 I 期 Young stage I	幼鱼 II 期 Young stage II	成鱼 I 期 Adult stage I	成鱼 II 期 Adult stage II
组织体积 TV/mm <sup>3</sup>	0.159±0.006 <sup>a</sup>	1.207±0.009 <sup>a</sup>	20.442±4.224 <sup>b</sup>	117.080±0.749 <sup>c</sup>
骨体积 BV/mm <sup>3</sup>	0.119±0.003 <sup>a</sup>	0.877±0.014 <sup>a</sup>	12.243±0.471 <sup>b</sup>	101.235±0.698 <sup>c</sup>
骨体积分数 BV/TV/%	74.857±0.943 <sup>ab</sup>	72.720±0.628 <sup>ab</sup>	62.620±13.223 <sup>a</sup>	86.473±1.029 <sup>b</sup>
骨小梁数量 Tb.N/(ind./mm)	19.915±0.758 <sup>d</sup>	10.115±0.290 <sup>c</sup>	4.341±0.107 <sup>b</sup>	1.960±0.043 <sup>a</sup>
骨小梁厚度 Tb.Th/mm	0.060±0.001 <sup>a</sup>	0.105±0.004 <sup>b</sup>	0.254±0.003 <sup>c</sup>	0.718±0.026 <sup>d</sup>
骨小梁分离度 Tb.Sp/mm	0.068±0.004 <sup>a</sup>	0.106±0.010 <sup>a</sup>	0.206±0.006 <sup>b</sup>	0.402±0.029 <sup>c</sup>
骨表面积 BS/mm <sup>2</sup>	0.887±0.090 <sup>a</sup>	7.958±0.449 <sup>a</sup>	79.175±7.980 <sup>b</sup>	179.551±14.606 <sup>c</sup>
骨表面积和骨体积之比 BS/BV/(ind./mm)	8.767±0.633 <sup>c</sup>	9.815±0.717 <sup>c</sup>	6.741±0.855 <sup>b</sup>	1.814±0.157 <sup>a</sup>
骨矿物质密度 BMD/(mg/mL)	820.527±5.003 <sup>d</sup>	707.532±2.201 <sup>b</sup>	678.052±4.417 <sup>a</sup>	743.855±0.307 <sup>c</sup>
组织矿物质密度 TMD/(mg/mL)	636.001±7.432 <sup>b</sup>	564.469±1.332 <sup>ab</sup>	460.300±102.825 <sup>a</sup>	654.797±7.031 <sup>b</sup>

注：同一指标不同字母代表差异显著( $P<0.05$ )，下同。

Note: Different letters of the same index represent significant difference ( $P<0.05$ ). The same below.

表3 4个不同发育期虹鳟脊椎骨中钙磷元素含量

Tab.3 Comparison of calcium and phosphorus contents in vertebrae of *O. mykiss* at four different developmental stages

指标 Index	幼鱼 I 期 Young stage I	幼鱼 II 期 Young stage II	成鱼 I 期 Adult stage I	成鱼 II 期 Adult stage II
钙 Ca /( $\mu\text{mol/g}$ )	2 407.686±291.485 <sup>a</sup>	4 711.121±567.948 <sup>b</sup>	4 461.943±543.106 <sup>b</sup>	3 794.687±802.197 <sup>ab</sup>
磷 P /( $\mu\text{mol/g}$ )	2 060.279±258.932 <sup>a</sup>	3 649.488±446.961 <sup>b</sup>	3 262.772±392.678 <sup>ab</sup>	2 695.399±514.384 <sup>ab</sup>
钙/磷质量比 Ca/P mass ratio	1.622±0.008 <sup>a</sup>	1.791±0.013 <sup>b</sup>	1.897±0.006 <sup>c</sup>	1.944±0.051 <sup>c</sup>
钙/磷(摩尔质量比值) Ca/P molar mass ratio	1.169±0.006 <sup>a</sup>	1.291±0.010 <sup>b</sup>	1.367±0.005 <sup>c</sup>	1.401±0.037 <sup>d</sup>

*molitrix*)为 1.25 (郭洪壮等, 2020)。由此可见, 骨骼中钙、磷元素的含量也可作为物种鉴别的依据之一。本研究中, 虹鳟脊椎骨的钙、磷含量在生长发育过程中呈先升高后降低的趋势, 表明骨骼矿化程度与年龄密切相关。由此可推测, 骨骼钙、磷元素的含量在鱼类年龄鉴定研究中也具有一定的应用意义。

鱼类骨骼的形态结构在不同发育时期也可能会发生变化, 相关特征在鱼类年龄鉴定研究中具有潜在应用价值。本研究利用 Micro-CT 扫描技术对 4 个不同发育期虹鳟第 4~6 节脊椎骨的扫描及重建结果显示(图 2A~H 和图 3A~D), 虹鳟脊椎骨大小在生长发育过程中显著增加( $P<0.05$ ), 同时伴随着脊椎骨间隙减小及脊椎骨表面结构的明显变化; 此外, TV、BV、BV/TV 和 BS(骨表面积)等随虹鳟的生长发育显著升高( $P<0.05$ ); 脊椎骨 BMD 在幼鱼 I 期显著高于其他发育时期( $P<0.05$ )。上述结果表明, 其脊椎骨结构指标在发育过程中变化显著。推测其原因可能是骨骼在生长发育的不同时期承受功能(运动)负荷的差异所致。

已有研究表明, 持续游动可显著提高鱼类骨骼强度( $P<0.05$ )。例如, 持续游动可显著提高虹鳟脊椎骨的矿物质含量和骨细胞密度(Totland *et al.*, 2011)、提

高大西洋鲑的骨骼强度(Ytteborg *et al.*, 2013); 游动对斑马鱼(*Brachydanio rerio* var)尾椎骨的成骨细胞活性、钙含量、数量和表面积、骨矿化程度以及 TV、BV 等显微结构指标均有显著影响(Suniaga *et al.*, 2018)。此外, 大黄鱼野生群体脊椎骨的 BV/TV、BMD 和 TMD 等骨骼强度评价指标均显著高于养殖群体( $P<0.05$ ), 推测其原因可能是野生群体需进行大量游动以完成索饵和躲避敌害等行为(王映等, 2016); 在鲤鱼游动的重要组织(背鳍、腹鳍和尾鳍)的骨骼中, 骨质矿物质含量、BMD 和 BV/TV 等均高于其他组织(张宁等, 2012)。上述研究表明, 硬骨鱼类骨骼的显微结构及矿化程度与其功能(游动)密切相关, 尤其是在脊椎骨中, 持续的游泳运动可诱导鱼类脊椎骨加速矿化。

本研究中, 骨小梁空间形态结构评价指标 Tb.N 随着虹鳟的生长发育显著降低( $P<0.05$ ), 而 Tb.Th 和 Tb.Sp 在发育过程中均呈显著升高的趋势( $P<0.05$ ), 上述结果表明, 虹鳟脊椎骨的骨小梁空间形态结构在发育过程中变化显著。据报道, 鱼类骨骼的骨小梁空间形态结构与功能(运动)也密切相关。例如, 在鲤鱼机体负荷较大的头部骨骼、背鳍和尾鳍等部位 Tb.N

较小,在背鳍、腹鳍和尾鳍等利于稳定其体质量分布的区域中 Tb.Th 较高(张宁等, 2012)。在运动强度较大的野生群体中, 大黄鱼骨骼的 Tb.Sp 较低(王映等, 2016)。然而, 上述骨骼显微结构检测指标可否应用于鱼类年龄鉴定、群体鉴定及分类鉴定等工作还有待进一步研究。

#### 4 结论

本研究利用软骨-硬骨双染色法和 X 射线扫描技术分别对虹鳟稚鱼和成鱼全骨骼形态进行系统观察, 明确了虹鳟脊椎骨的形态特征。随后, 利用 Micro-CT 及 ICP-MS 技术分别对 4 个不同发育期虹鳟脊椎骨进行三维结构扫描、显微结构指标分析及钙、磷元素含量检测。结果表明, TV、BV、BV/TV、BS、Tb.Th 和 Tb.Sp 等骨骼空间形态结构的评价指标在虹鳟生长发育过程中显著增加, Tb.N 显著降低; 骨骼强度评价指标 BMD 则呈现先降低后升高的趋势。脊椎骨显微结构在不同发育期的显著差异可能与其功能性密切相关。虹鳟脊椎骨中钙、磷元素含量在不同发育期呈先升高后降低的趋势, 钙/磷(摩尔质量比值)随虹鳟的生长呈显著增加趋势, 表明骨骼矿化程度随生长发育不断增加。由此可见, 脊椎骨显微结构指标及其中的钙、磷元素含量在鱼类年龄鉴定研究中具有潜在应用价值, 此外, 上述指标在应用于鱼类群体鉴定及分类鉴定等工作时需考虑年龄因素的影响。

#### 参 考 文 献

- AKHAN S, OKUMU, SONAY F D, *et al.* Growth, slaughter yield and proximate composition of rainbow trout (*Oncorhynchus mykiss*) raised under commercial farming condition in Black Sea. Kafkas Universitesi Veteriner Fakultesi Dergisi, 2010, 16: 179–182
- AN X, LI Z R, WANG J L, *et al.* Micro-CT imaging of angiogenesis in rats with knee osteoarthritis. Academic Journal of Chinese PLA Medical School, 2018, 39(6): 533–537, 550 [安晓, 李志锐, 王俊良, 等. 大鼠膝关节炎模型血管增生显微 CT 观察. 解放军医学院学报, 2018, 39(6): 533–537, 550]
- BORDIGNON F, GASCO L, BIROLO M, *et al.* Performance and fillet traits of rainbow trout (*Oncorhynchus mykiss*) fed different levels of *Hermetia illucens* meal in a low-tech aquaponic system. Aquaculture, 2022, 546: 737279
- BOUXSEIN M L, BOYD S K, CHRISTIANSEN B A, *et al.* Guidelines for assessment of bone microstructure in rodents using micro-computed tomography. Journal of Bone and Mineral Research, 2010, 25(7): 1468–1486
- CAMP A L. A neck-like vertebral motion in fish. Proceedings of the Royal Society B: Biological Sciences, 2021, 288(1957): 20211091
- CAO X D. Technology of feeding rainbow trout in flowing water. Henan Fisheries, 2017(6): 8–9 [曹祥栋. 虹鳟流水养殖技术. 河南水产, 2017(6): 8–9]
- CHEN Y X, LIU J, LIU L. Comparative osteology in eight sparid fishes (Osteichthyes: Perciformes) with remarks on their classification. Journal of Fisheries of China, 2014, 38(9): 1360–1374 [陈咏霞, 刘静, 刘龙. 中国鲷科鱼类骨骼系统比较及属种间分类地位探讨. 水产学报, 2014, 38(9): 1360–1374]
- DESCHAMPS M H, KACEM A, VENTURA R, *et al.* Assessment of silent vertebral abnormalities, bone mineralization and bone compactness in farmed rainbow trout. Aquaculture, 2008, 279(1/2/3/4): 11–17
- DESCHAMPS M H, LABBÉ L, BALOCHE S, *et al.* Sustained exercise improves vertebral histomorphometry and modulates hormonal levels in rainbow trout. Aquaculture, 2009, 296(3/4): 337–346
- DINGERKUS G, UHLER L D. Enzyme clearing of alcian blue stained whole small vertebrates for demonstration of cartilage. Stain Technology, 1977, 52(4): 229–232
- FELDKAMP L A, GOLDSTEIN S A, PARFITT A M, *et al.* The direct examination of three-dimensional bone architecture in vitro by computed tomography. Journal of Bone and Mineral Research, 1989, 4(1): 3–11
- FJELLDAL P G, HANSEN T, BRECK O, *et al.* Vertebral deformities in farmed Atlantic salmon (*Salmo salar* L.) -etiology and pathology. Journal of Applied Ichthyology, 2012, 28(3): 433–440
- GUO H Z, HU Y M, WANG H, *et al.* Composition of calcium in the bones of four major Chinese carps. Food and Fermentation Industries, 2020, 46(18): 226–231 [郭洪壮, 胡月明, 王辉, 等. “四大家鱼”鱼骨钙的组成分析. 食品与发酵工业, 2020, 46(18): 226–231]
- HU J, LIU Y, YU G, *et al.* Osteological development of the vertebral column and caudal complex in larval and juvenile blackhead seabream, *Acanthopagrus schlegelii* (Perciformes, Sparidae)(Bleeker, 1854). Pakistan Journal of Zoology, 2019, 51(5): 1859–1867
- HUANG D Y, TAO M J, ZHI H B. Determination of 13 trace elements in high-purity chromium by ICP-MS. Physical Testing and Chemical Analysis Part B: Chemical Analysis, 2021, 57(8): 759–763 [黄丹宇, 陶美娟, 郅惠博. 电感耦合等离子体质谱法测定高纯铬中 13 种痕量元素. 理化检验(化学分册), 2021, 57(8): 759–763]
- HUBER H R, JORGENSEN J C, BUTLER V L, *et al.* Can salmonids (*Oncorhynchus* spp.) be identified to species using vertebral morphometrics? Journal of Archaeological Science, 2011, 38(1): 136–146
- JAGIELŁO K, POLONIS M, OCALEWICZ K. Incidence of skeletal deformities in induced triploid rainbow trout (Walbaum, 1792). Oceanological and Hydrobiological Studies,

- 2021, 50(2): 150–159
- LI X H, TANG Y T, TIAN F, *et al.* Morphological analysis used by geometric morphometrics combined with micro CT among *Gymnocypris eckloni* in two drainage (Teleostei: Cyprinidae). *Acta Hydrobiologica Sinica*, 2020, 44(4): 853–861 [李晓慧, 汤永涛, 田菲, 等. 几何形态测量法结合 Micro CT 扫描对两水系花斑裸鲤的形态分析. *水生生物学报*, 2020, 44(4): 853–861]
- LIANG J J. Mineral nutrition of juvenile grass carp (*Ctenopharyngodon idella*). Doctoral Dissertation of Sun Yat-Sen University, 2012 [梁键钧. 草鱼幼鱼的矿物质营养研究. 中山大学博士研究生学位论文, 2012]
- LIU G P. Micro CT principal and application. *Journal of Tissue Engineering and Reconstructive Surgery*, 2006, 2(4): 228–229 [刘广鹏. MicroCT 原理及应用. *组织工程与重建外科杂志*, 2006, 2(4): 228–229]
- MARKVART M, DARVANN T A, LARSEN R, *et al.* Micro-CT analyses of apical enlargement and molar root canal complexity. *International Endodontic Journal*, 2012, 45(3): 273–281
- MENG Q W, SU J X, LI W D. Comparative anatomy of fishes. Beijing: Science Press, 1987, 57–118 [孟庆闻, 苏锦祥, 李婉端. 鱼类比较解剖. 北京: 科学出版社, 1987, 57–118]
- PINTO M, JEPSEN K J, TERRANOVA C J, *et al.* Lack of sexual dimorphism in femora of the eusocial and hypogonadic naked mole-rat: A novel animal model for the study of delayed puberty on the skeletal system. *Bone*, 2010, 46(1): 112–120
- SAKASHITA M, SATO M, KONDO S. Comparative morphological examination of vertebral bodies of teleost fish using high-resolution micro-CT scans. *Journal of Morphology*, 2019, 280(6): 778–795
- SÖNMEZ A Y, BİLEN S, TAŞTAN Y, *et al.* Oral administration of *Sargassum polycystum* extracts stimulates immune response and increases survival against *Aeromonas hydrophila* infection in *Oncorhynchus mykiss*. *Fish and Shellfish Immunology*, 2021, 117: 291–298
- SUNIAGA S, ROLVIEN T, SCHEIDT A V, *et al.* Increased mechanical loading through controlled swimming exercise induces bone formation and mineralization in adult zebrafish. *Scientific Reports*, 2018, 8(1): 1–13
- TOTLAND G K, FJELLDAL P G, KRYVI H, *et al.* Sustained swimming increases the mineral content and osteocyte density of salmon vertebral bone. *Journal of Anatomy*, 2011, 219(4): 490–501
- WANG J, PENG J, TAN Z, *et al.* Microplastics in the surface sediments from the Beijiang River littoral zone: Composition, abundance, surface textures and interaction with heavy metals. *Chemosphere*, 2017, 171: 248–258
- WANG S, ZHANG J, MA X X, *et al.* Determination of the contents of 12 metallic elements in seafood by ICP-MS. *Journal of Chinese Institute of Food Science and Technology*, 2010, 10(6): 204–207 [王硕, 张佳, 马晓星, 等. ICP-MS 法测定海产品中 12 种金属元素的含量. *中国食品学报*, 2010, 10(6): 204–207]
- WANG Y, ZHAO J L, KE Q Z. Comparison of bone microstructures in cultured and wild stocks of large yellow croaker (*Larimichthys crocea*) using micro CT scanning. *Marine Sciences*, 2016, 40(12): 36–40 [王映, 赵金良, 柯巧珍. 大黄鱼养殖群体和野生群体骨骼 micro CT 扫描显微结构比较. *海洋科学*, 2016, 40(12): 36–40]
- WEI Z Y, ZHANG Z L. Interpretation and application of micro-CT to obtain microstructure index in bone metabolism research. *Chinese Journal of Osteoporosis and Bone Mineral Research*, 2018, 11(2): 200–205 [魏占英, 章振林. Micro-CT 在骨代谢研究中骨微结构指标的解读及应用价值. *中华骨质疏松和骨矿盐疾病杂志*, 2018, 11(2): 200–205]
- XIE X, BAO Z Y, WANG Q Z. Advances of fish age identification. *Journal of Dalian Ocean University*, 2021, 36(6): 1071–1080 [谢玺, 鲍积月, 王庆志. 鱼类年龄硬组织鉴定方法研究应用进展. *大连海洋大学学报*, 2021, 36(6): 1071–1080]
- YTTEBORG E, TORGERSEN J S, PEDERSEN M E, *et al.* Exercise induced mechano-sensing and substance P mediated bone modeling in Atlantic salmon. *Bone*, 2013, 53(1): 259–268
- ZENG T, SHEN Q. The application progress of inductively coupled plasma mass spectrometry. *Guangdong Chemical Industry*, 2018, 45(18): 116, 119 [曾涛, 沈倩. 电感耦合等离子体质谱法(ICP-MS)应用进展及展望. *广东化工*, 2018, 45(18): 116, 119]
- ZHANG N, SU S Y, DONG Z J. Study on bone and microstructure of common carp using micro CT scanning. *South China Fisheries Science*, 2012, 8(6): 44–49 [张宁, 苏胜彦, 董在杰. 基于 micro CT 扫描技术的鲤骨骼和显微结构分析. *南方水产科学*, 2012, 8(6): 44–49]
- ZHANG Y, PENG X F. Micro-CT scanning analysis for inner structure of porous media. *Journal of Engineering Thermophysics*, 2005, 26(5): 850–852 [张扬, 彭晓峰. 多孔材料内部结构的微 CT 扫描仪分析. *工程热物理学报*, 2005, 26(5): 850–852]
- ZHENG H Y, GUO X Q, ZHU Z X, *et al.* Determination of Cu, Cd, Cr and Zn in fish and shrimp by automated graphite digestion combined with inductively coupled plasma mass spectrometry. *Journal of Food Safety and Quality*, 2017, 8(1): 270–274 [郑红艳, 郭雪勤, 朱志勋, 等. 全自动石墨消解-电感耦合等离子体质谱测定鱼、虾等生物样品中铜、镉、锌、铬 4 种重金属元素. *食品安全质量检测学报*, 2017, 8(1): 270–274]
- ZHOU Q L, WANG L Y, ZHAO X L, *et al.* Effects of salinity acclimation on histological characteristics and miRNA expression profiles of scales in juvenile rainbow trout (*Oncorhynchus mykiss*). *BMC Genomics*, 2022, 23(1): 1–15



## Calcium and Phosphorus Contents, and Microstructure of Vertebrae in Rainbow Trout (*Oncorhynchus mykiss*) at Different Developmental Stages

ZHOU Qiling<sup>1</sup>, WANG Liuyong<sup>1</sup>, YANG Yunsheng<sup>1</sup>, MA Qian<sup>1,2①</sup>, WU Yuwei<sup>1</sup>, CHEN Gang<sup>1,2</sup>

(1. College of Fisheries, Guangdong Ocean University, Zhanjiang 524088, China;

2. Southern Marine Science and Engineering Guangdong Laboratory (Zhanjiang), Zhanjiang 524025, China)

**Abstract** The skeletal system of fish consists of the axial skeleton (skull, vertebral column, ribs, and intermuscular bones) and the appendicular skeleton, which are essential for behavioral and physiological functions such as locomotion, feeding, predator avoidance, and load-bearing. As for the vertebral column of teleosts, it is composed of many vertebrae connected from the head to the caudal base. The morphological characteristics of the vertebrae (such as the number and structure) vary among different fish species. These characters (especially the vertebrae number) provide an important basis for species identification. For instance, the number of vertebrae in *Salmo salar* is 57–60 (30 trunk vertebrae, 27–30 caudal vertebrae), while rainbow trout (*Oncorhynchus mykiss*) has a total of 63 vertebrae (including 33 trunk vertebrae and 30 caudal vertebrae), which can be used for species identification. Fish with a similar number of vertebrae require further skeletal morphological features to distinguish them. For instance, the three-dimensional structure of the same vertebra segment from 32 different teleost species (belonging to 10 different orders) were compared and analyzed using Micro-computed tomography (Micro-CT) scanning technology. The results showed that the lamellar trabeculae and its internal cavity structure on the spine differed between the species, suggesting that these structural characteristics can serve as additional evidence to classify and identify fish species. In addition, calcium (Ca) and phosphorus (P) are the most important mineral elements in a fish skeleton, and their contents vary among different fish. Therefore, there is potential to use the skeletal Ca and P contents in classifying and identifying fish and their life history characteristics.

To examine the vertebrae number in *O. mykiss*, specimens of juvenile *O. mykiss* of body weight (1.27±0.21) g were cleaned and double-stained to obtain the whole skeletal image. A total of 63 vertebrae were identified, and all were completely ossified at this developmental stage. X-ray scanner technology scanned and photographed the entire skeletal structure of adult *O. mykiss*. The adult results were similar to the juvenile results of 63 vertebrae with both ends connected with the head or tail, and the ribs were attached to the trunk vertebrae. The ventral sides of the 1–33 trunk vertebrae were arranged in an arc, which was downward and separate. No intermuscular spine was evident. On the dorsal side of the vertebrae, the neural arches surrounding the neural canal were fused with the neural spines. Unlike the ribs, the caudal vertebrae had vascular arches, which formed passages for blood vessels and nerves and were fused with the vascular spines on the ventral side.

The calcium and phosphorus content, and microstructure of the vertebrae in *O. mykiss* at different developmental stages were assessed. Vertebrae samples were collected at four developmental stages (young stage I, young stage II, adult stage I, and adult stage II; with an average body weight of 4, 35, 644 and 2 129 g, respectively). The calcium and phosphorus contents in the 1–6th vertebrae were assessed by inductively coupled plasma mass spectrometry (ICP-MS). The 4–6th vertebrae were scanned using

① Corresponding author: MA Qian, E-mail: maq@gdou.edu.cn

Micro-CT technology. The results revealed the calcium and phosphorus contents of the vertebrae initially increased and then decreased during development. The highest levels of calcium and phosphorus in the vertebrae was at young stage II, ( $4\ 711.121\pm 567.948$ ) and ( $3\ 649.488\pm 446.961$ )  $\mu\text{mol/g}$ , respectively. The Ca/P molar mass ratio increased significantly with the growth of *O. mykiss* ( $P<0.05$ ). These results indicated that the degree of mineralization in the vertebrae increased with growth and development. Micro-CT scanning results indicated that the bone volume and surface of the vertebrae increased significantly with the growth of *O. mykiss*. The vertebrae segments became more obvious, and the structure became more complete. The vertebral microstructure indexes in *O. mykiss* at the different developmental stages suggested the trabecular number (Tb.N) significantly decreased with the growth of *O. mykiss* ( $P<0.05$ ). The highest levels occurred at young stage I with ( $19.915\pm 0.758$ ) ind./mm, the lowest levels occurred at adult stage II with ( $1.960\pm 0.043$ ) ind./mm. The trabecular thickness (Tb.Th) and trabecular separation/spacing (Tb.Sp), both significantly increased with *O. mykiss* growth ( $P<0.05$ ). Tb.Th and Tb.Sp of the vertebrae in *O. mykiss* were the lowest, ( $0.060\pm 0.001$ ) mm and ( $0.068\pm 0.004$ ) mm, respectively at young stage I, and the highest levels, ( $0.718\pm 0.026$ ) mm and ( $0.402\pm 0.029$ ) mm, respectively) were at adult stage II. In addition, the bone volume fraction (BV/TV), tissue mineral density (TMD), and bone mineral density (BMD) showed a trend of initially decreasing and then increasing. The lowest levels were at adult stage I, ( $62.620\pm 13.223$ )%, ( $460.300\pm 102.825$ ) mg/mL and ( $678.052\pm 4.417$ ) mg/mL, respectively, and the highest BV/TV and TMD, ( $86.473\pm 1.029$ )% and ( $654.797\pm 7.031$ ) mg/mL were at adult stage II. Conversely, the highest BMD, ( $820.527\pm 5.003$ ) mg/mL, was at young stage I. The evaluation indexes of the bone spatial morphological structures (such as TV, BV, BV/TV, BS, Tb.Th, and Tb.Sp) increased significantly during the growth and development of rainbow trout, while Tb.N decreased significantly. The bone strength evaluation index, BMD initially decreased and then increased. The significant variation in the vertebra microstructure at the different developmental stages might be closely related to its function. These results indicate that the microstructure and element contents of vertebrae in *O. mykiss* changes significantly during development and the relative results could provide more reliable data for age, group, and taxonomic identification of fish.

**Key words** *Oncorhynchus mykiss*; Vertebrae; Growth and development; Microstructure; Element content